Journal of Materials Chemistry

Cite this: *J. Mater. Chem.*, 2011, **21**, 10532

www.rsc.org/materials

PAPER

Thiophene–benzothiadiazole–thiophene (D–A–D) based polymers: effect of donor/acceptor moieties adjacent to D–A–D segment on photophysical and photovoltaic properties†

Prashant Sonar,* Evan L. Williams, Samarendra P. Singh and Ananth Dodabalapur‡*

Received 14th February 2011, Accepted 20th April 2011
DOI: 10.1039/c1jm10649j

New push–pull copolymers based on thiophene (donor) and benzothiadiazole (acceptor) units, poly[4,7-bis(3-dodecylthiophene-2-yl) benzothiadiazole-*co*-thiophene] (**PT3B1**) and poly[4,7-bis(3-dodecylthiophene-2-yl) benzothiadiazole-*co*-benzothiadiazole] (**PT2B2**), are designed and synthesized *via* Stille and Suzuki coupling routes respectively. Gel permeation chromatography shows the number average molecular weights are 31 100 and 8400 g mol^{-1} for the two polymers, respectively. Both polymers have shown absorption throughout a wide range of the UV-vis region, from 300 to 650 nm. A significant red shift of the absorption edge is observed in thin films compared to solution of the copolymers; the optical band gap is in the range of 1.7 to 1.8 eV. Cyclic voltammetry indicates reversible oxidation and reduction processes with HOMO energy levels calculated to be in the range of 5.2 to 5.4 eV. Upon testing both materials for organic field-effect transistors (OFETs), **PT3B1** showed a hole mobility of 6.1×10^{-4} cm^2 V^{-1} s^{-1}, while **PT2B2** did not show any field effect transport. Both copolymers displayed a photovoltaic response when combined with a methanofullerene as an electron acceptor. The best performance was achieved when the copolymer **PT3B1** was blended with [70]PCBM in a 1 : 4 ratio, exhibiting a short-circuit current of 7.27 mA cm^{-2}, an open circuit voltage of 0.85 V, and a fill factor of 41% yielding a power conversion efficiency of 2.54% under simulated air mass (AM) 1.5 global (1.5 G) illumination conditions (100 mW cm^{-2}). Similar devices utilizing **PT2B2** in place of **PT3B1** demonstrated reduced performance with a short-circuit current of 4.8 mA cm^{-2}, an open circuit voltage of 0.73 V, and a fill factor of 30% resulting in a power conversion efficiency of roughly 1.06%.

1. Introduction

Conjugated semiconducting polymers, oligomers, and small molecules are an important class of materials for the development of printable and flexible electronics.[1] These materials have drawn significant attention over the last two decades for a variety of organic electronic device applications [organic light emitting diodes (OLEDs), organic field effect transistors (OFETs) and organic photovoltaics (OPVs)] due to their tuneable optical and electrical characteristics.[2–4] In such devices, active layers of the semiconducting materials on the order of 20–100 nm can be deposited between two electrodes and the optoelectronic properties can be investigated. Photophysical and electrochemical properties of these conjugated materials are primarily controlled by the modulation in chemical structures through changes in the conjugation backbone which allows for band gap tuning. Of these materials, low band-gap conjugated materials are of particular interest because of their utility in harvesting visible and near infrared wavelength photons and possible ambipolar charge transport properties in electronic devices.[5] One of the successful and elegant approaches to making low band gap materials is the incorporation of strong electron donating and electron accepting moieties [push–pull system] along the conjugated backbone.[6] The alternating donor and acceptor arrangement causes the hybridization of the highest occupied molecular orbital (HOMO) of the donor with lowest unoccupied molecular orbital (LUMO) of the acceptor and results in a reduction of the band gap. The incorporation of a conjugated heterocyclic unit can greatly influence the optical, electrochemical, morphological and electrical properties of conjugated materials.[7] Additionally, this incorporation may enhance the intramolecular charge transfer, which in turn can improve the charge carrier mobility. The utilization of thiophene as a donating moiety and 2,1,3-benzothiadiazole as an accepting moiety is a well-studied and successful strategy for making low band gap materials.[8–12] Furthermore, nitrogen

*Institute of Materials Research and Engineering, Agency for Science, Technology, and Research (A*STAR), 3 Research Link, Singapore, 117602, Republic of Singapore. E-mail: sonarp@imre.a-star.edu.sg; ananth.dodabalapur@engr.utexas.edu*

† Electronic supplementary information (ESI) available. See DOI: 10.1039/c1jm10649j

‡ Permanent address: Microelectronics Research Center, University of Texas at Austin, Austin, TX, 78758, USA.

based heterocycles such as thiazole, thiadiazole, pyrazine and their derivatives incorporated with thiophene in the conjugated backbone have shown non-covalent sulfur–nitrogen (S···N) interactions within the molecule. These interactions influence molecular assembly in the solid state.[13] In an earlier report, we successfully synthesized thiophene–benzothiadiazole based alkyl end capped solution processable donor–acceptor (D–A) conjugated small molecules with varying ratios of thiophene and benzothiadiazole.[14] In these materials, we observed the energy levels, liquid crystallinity, and thin film morphological properties to all be influenced by the ratio of the donor–acceptor moiety. Following successful utilization of these D–A small molecules in solution-processed OFETs, we decided to synthesize analogous copolymers of these model compounds in order to study structure–property relationships and performance in both OFET and OPV devices. Polymers often display better thin film-forming characteristics through various solution-based processing techniques such as spin coating, dip coating and ink-jet printing, than small molecules, which offer greater promise in terms of printing organic electronic devices.[15] Conjugated polymers comprising donor–acceptor blocks are an interesting system to use as a tool to study the effect of materials design, energy levels and optical shifts on the performance in bulk heterojunction (BHJ) OPV devices. Whereas in OFET devices, it is particularly interesting to study the charge transporting properties of these D–A materials through variations in designing such as strength of donor and acceptor units used in the conjugated backbone, their location relative to each other and the overall planarity.

There are reports of using a thiophene–benzothiadiazole–thiophene segment with a variety of other comonomers such as indenofluorene,[11a] thienothiophene,[11b,c] cyclopentadithiophene,[9a] fluorene,[10] carbazole,[9b,c] dibenzosilole[8b,c] and longer oligothiophenes to yield low band gap copolymers.[12] The thiophene–benzothiadiazole–thiophene has thus been established as a promising segment which can be attached with other novel and interesting donor/acceptor conjugated units to make a library of copolymers with tailored photophysical properties. It is well known that a polymer's molecular weight, solubility, thin film morphology, crystallinity, band gap, and charge carrier mobility are important parameters which may have great influence on the device performance. In this article, we report the design and synthesis of two donor–acceptor based copolymers poly[4,7-bis-(3-dodecylthiophene-2-yl) benzothiadiazole-*co*-thiophene] (**PT3B1**) and poly[4,7-bis(3-dodecylthiophene-2-yl) benzothiadiazole-*co*-benzothiadiazole] (**PT2B2**). A thiophene–benzothiadiazole–thiophene segment with either a thiophene or benzothiadiazole comonomer is correspondingly used for making these copolymers, with the objective to investigate the effect of adjacent donor and acceptor comonomer units on optoelectronic properties. These materials were characterized by NMR spectroscopy, gel permeation chromatography, UV-Vis absorption and photoluminescence spectroscopy, thermogravimetric analysis and cyclic voltammetry. OFETs made from **PT3B1** on octyltrichlorosilane (OTS) treated Si/SiO_2 substrate showed hole mobilities of 6.1×10^{-4} cm^2 V^{-1} s^{-1} using gold for source and drain electrodes. Bulk heterojunction OPV devices were fabricated by blending the donor copolymer with [6,6] phenyl-C71-butyric acid methyl ester ($PC_{70}BM$) as the acceptor. The highest achieved power conversion efficiencies were 2.5% and 1%, using a polymer to fullerene ratio of 1 : 4 for **PT3B1** and **PT2B2**, respectively. The detailed synthesis, characterization, and correlation of structure to device performance are discussed herein.

2. Results and discussion

2.1 Syntheses and characterization

The synthetic strategy for making the soluble version of thiophene–benzothiadiazole–thiophene segment is outlined in Scheme 1. In order to provide good solubility of the polymer, a dodecyl group was introduced on thiophene. First, commercially available 3-dodecyl thiophene (**1**) was brominated at the 2-position by using *N*-bromosuccinamide (NBS) in a mixture of chloroform and acetic acid (1 : 1) solvent providing the 2-bromo-3-dodecyl thiophene (**2**) (93% yield). Selective stannylation at the 2-position of 3-dodecyl thiophene was carried out by synthesizing intermediate Grignard reagent (GR) using magnesium turnings in dry tetrahydrofuran (THF). After the addition of tributyltin chloride at −78 °C in the above synthesized GR gave 2-tributyltin-3-dodecylthiophene (**3**) (61% yield). Compound **3** was then reacted (3 equivalents) with commercially available 4,7-dibromobenzo[*c*][1,2,5]thiadiazole in dry *N*,*N*-dimethylformamide (DMF) in the presence of $Pd(PPh_3)_4$ catalyst at 80 °C for 24 h by Stille coupling, which produced 4,7-bis(3-dodecylthiophene-2-yl)benzo[*c*][1,2,5]thiadiazole (**5**) (65% yield) after column chromatography. Bromination of compound **5** was carried out using NBS in DMF at room temperature for 24 h producing 4,7-bis(5-bromo-3-dodecylthiophen-2-yl)benzo[*c*]-[1,2,5]thiadiazole (**6**) (62% yield). This dibromo derivative (compound **6**) was used as a common block for polymerization with other two comonomers such as thiophene (donor) and benzothiadiazole (acceptor) respectively.

The synthesis of two new alternating copolymers comprised of three thiophene with one benzothiadiazole units (**PT3B1**) and two thiophene with two benzothiadiazole units in the conjugated backbone (**PT2B2**) is shown in Scheme 2. 2,5-Bi(trimethylstannyl)thiophene (**7**) and 4,7-bis(4,4,5,5-tetramethyl-1,3,2-dioxabrolan-2-yl)benzothiadiazole (**8**) were synthesized

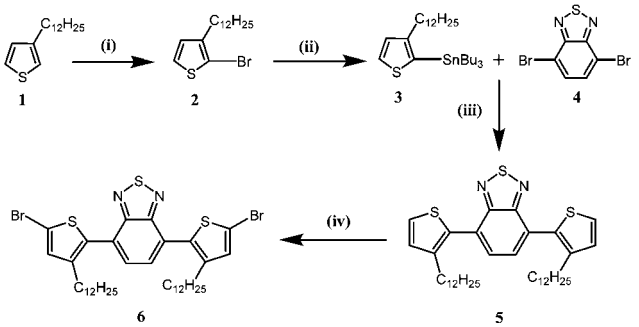

Scheme 1 *Reagents and conditions*: (i) *N*-bromosuccinamide, $CHCl_3$: CH_3COOH (1 : 1), room temp., overnight, 93%; (ii) magnesium turnings, anhydrous THF, reflux for 2 h, tributyltin chloride, −78 °C, overnight, 83%; (iii) $Pd(PPh_3)_4$, anhydrous DMF, 81%; (iv) *N*-bromosuccinamide, DMF, 24 h, 88%.

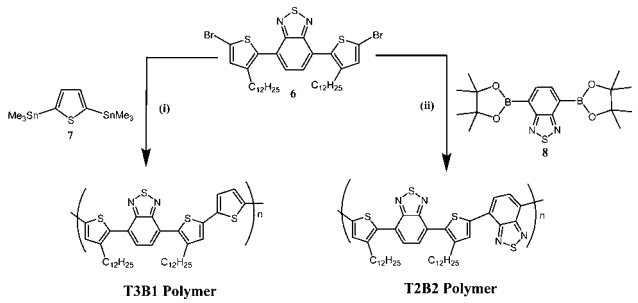

Scheme 2 *Reagents and conditions*: (i) $Pd_2(dba)_3$, P(*o*-tolyl)$_3$P, chlorobenzene, reflux, 120 °C, 72 h, 90%; (ii) Aliquat 336, $Pd(PPh_3)_4$, 2 M K_2CO_3, toluene, reflux, 48 h, 87%.

according to a reported procedure.[16] Compounds **6** and **7** were reacted in a Schlenk flask using tris(dibenzylideneacetone)-dipalladium(0) (Pd_2dba_3), tri(*o*-tolyl) phosphine [P(*o*-tol)$_3$] as the catalytic system in chlorobenzene solvent and then refluxed at 110 °C under argon atmosphere for 72 h *via* Stille coupling. After completion of the copolymerization, the polymer **PT3B1** was precipitated out in methanol. Another copolymerization was carried out at 80 °C under argon atmosphere for 72 h using compounds **6** and **8** in the presence of $Pd(PPh_3)_4$ as a catalyst, and 2 M K_2CO_3 as a base in toluene *via* Suzuki coupling. The reaction was terminated by adding the bromobenzene and phenyl boronic acid, respectively, and stirred additionally for another 5 h. The resulting mixture was poured into a mixture of methanol and 2 M HCl and stirred for few hours to precipitate the polymer. Such a non-solvent precipitation is a common method to recover the polymer sample *e.g.* polythiophene dilute solution in organic solvent can be precipitated either in methanol or acetone antisolvent. Both crude polymers were then subjected to purification using Soxhlet extraction for 2 days using methanol, acetone, and hexane solvents, respectively, for the removal of oligomer and catalytic impurities. The residue was finally extracted with chloroform and precipitated again from methanol, filtered, washed with methanol and dried. Purified polymers **PT3B1** and **PT2B2** showed the number average molecular weights (M_n) 31 100 g mol^{-1} and 8400 g mol^{-1} with polydispersity index (PDI) of 1.80 and 1.36, respectively, measured by Gel Permeation Chromatography (GPC) at a column temperature of 40 °C with THF as an eluent and polystyrene (PS) as standards. Both polymers are nicely soluble in many organic solvents such as THF, chloroform, toluene, chlorobenzene and dichlorobenzene. These polymers also exhibit nice film forming properties and large flakes of polymer films were obtained after precipitation in a non-solvent. The thermal stability of the polymers was analyzed by thermogravimetric analysis (TGA) under a nitrogen flow. **PT3B1** and **PT2B2** polymers show 5% weight loss at 449 °C and 433 °C, respectively, which indicates an excellent thermal stability of the materials. GPC and thermal data have been summarized in Table1. DSC characterization was carried out up to 300 °C but no thermal transition in the bulk sample was observed.

Table 1 Polymerization results and thermal stability of the copolymers

Polymers	M_n[a]/g mol^{-1}	M_w[b]/g mol^{-1}	PDI	T_d[c]
PT3B1	31 100	56 100	1.80	449
PT2B2	8400	11 500	1.36	433

[a] Number-average molecular weight. [b] Weight-average molecular weight equivalent to PS. [c] Decomposition temperature (with 5% weight loss) determined by TGA under N_2.

2.2 Optical properties

The absorption spectra of both the copolymers were measured in chloroform solutions (1×10^{-5} M based on repeat units) and are shown in Fig. 1a (Table 2). Both copolymers show absorption peaks in short and long wavelength regions. These peaks are related with the π–π* transition band and charge transfer transition between donor and acceptor blocks. The copolymer **PT3B1** shows short wavelength absorption peaks at 320 and 384 nm, respectively, which could be attributed to the oligothiophene segment. A longer wavelength peak is seen at 500 nm and is attributed to charge transfer associated with oligothiophene–benzothiadiazole (D–A) interaction.[11b,c,17] In the case of **PT2B2** peaks are located at 320 nm in short wavelength and 521 nm in longer wavelength regions. The peak at 320 nm is common in the absorption spectra of both **PT3B1** and **PT2B2** polymers, though weaker in the former. The peaks, in long and short wavelength regions, observed for both polymers are red shifted with respect to our earlier reported small molecule (**T3B1** and **T2B2**) model compounds.[14b] Such kinds of multiple absorption bands have been noticed in various donor–acceptor based conjugated

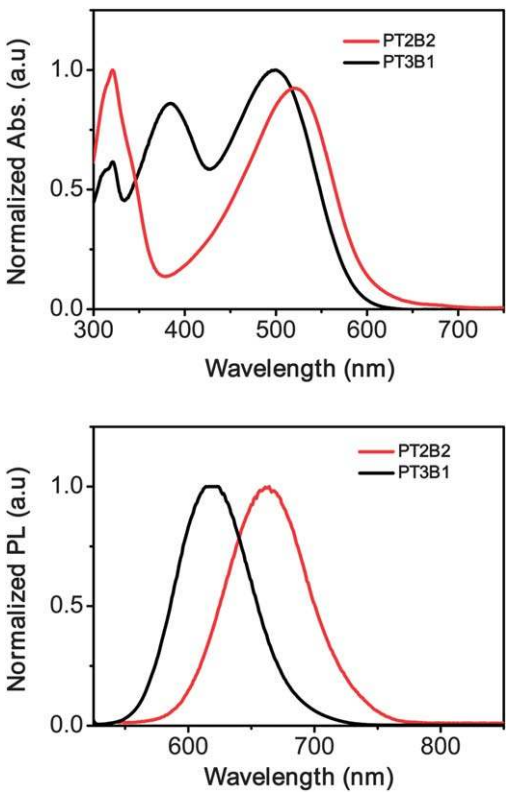

Fig. 1 (a) Normalized UV-vis and (b) emission spectrum of **PT3B1** and **PT2B2** in chloroform solution (10^{-5} M).

Table 2 Optical (UV-vis and PL) and electrochemical properties of the copolymers

Polymers	UV-Vis solution λ_{max}[a]/ nm	UV-Vis thin film λ_{max}[b]/ nm	Optical band gap[c]/ eV	PL solution in film λ_{max}[a]/ nm	HOMO[d]	LUMO[e]	Electrochemical band gap[f]/eV
PT3B1	384, 500	395, 539	1.80	618	5.20	3.24	1.96
PT2B2	320, 521	338, 589	1.71	662	5.40	3.60	1.80

[a] Diluted solution in chloroform. [b] Polymer film on a glass plate by spin coating from chloroform solution. [c] Optical band gap calculated from the absorption onset of the thin films. [d] Measured from the oxidation onset of the CV. [e] Obtained from the reduction onset of the CV. [f] Obtained from the HOMO–LUMO gap.

systems both in oligomers and polymers due to donor–acceptor orbital hybridization.[8–13] From the comparison of the optical data from both copolymers, it is clear that **PT2B2** shows a red shift of 21 nm (longer wavelength region) relative to **PT3B1**. This shift is attributed to the more extended delocalization of π-electrons due to the increased benzothiadiazole content in the D–A system. The increased benzothiadiazole content could lead to a stronger internal charge transfer interaction.[18] **PT3B1** shows a peak at 384 nm that is not observed in **PT2B2**. The origin/absence of this peak is not well understood, but it is clear that **PT2B2** lacks the adjacent thiophene units that are present in **PT3B1**.

The fluorescence spectra for both copolymers in chloroform are shown in Fig. 1b (Table 2). **PT3B1** and **PT2B2** copolymers exhibited weak red to dark red emission with maxima at 618 and 634 nm, respectively. It is highly expected that the weak fluorescence is due to the fast intramolecular charge transfer between donor and acceptor units after photoexcitation. The 16 nm red shift in emission for polymer **PT2B2**, compared to **PT3B1**, is attributed to the more extended conjugation of alternative thiophene–benzothiadiazole segments and the strong donor–acceptor interaction in the former. It is noteworthy that the difference in absorption and emission peaks is greater for **PT2B2** than for **PT3B1** (141 nm and 118 nm, respectively). From the optical data of both copolymers, it is evident that the donor–acceptor interaction in the backbone strongly depends on several factors *i.e.* strength of donors and acceptors, their attachment in backbone, steric hindrance between the blocks and planarity of the polymeric chains.

Solid state absorption measurements of these newly synthesized copolymers were compared with standard **P3HT**, widely used donor in the OPV system. **P3HT**, **PT3B1** and **PT2B2** thin films were processed by spin coating on glass from chloroform solution as shown in Fig. 2. In films, the peak bandwidth of the copolymers is broader and red shifted as compared to in solution. Solid state absorption maxima were recorded at 395 and 539 nm, for **PT3B1** films which is 11 nm and 39 nm red shifted, as compared to solution, in shorter and longer wavelength regions, respectively. Whereas in the case of **PT2B2**, the measured thin film absorption maxima at 338 and 589 nm are red shifted by18 nm and 68 nm, as compared to solution spectra. This red shift is associated with π–π stacking and interchain interactions of the polymeric chain in solid state. Optical band gaps, calculated from absorption cut off values, are determined to be 1.78 and 1.71 eV for **PT3B1** and **PT2B2** respectively (these values are lowered by 0.25 and 0.50 eV than **T3B1** and **T2B2** small molecule model compounds reported earlier[14b]). Materials with such a low band gap and wide absorption range are expected to have potential for OPV devices.

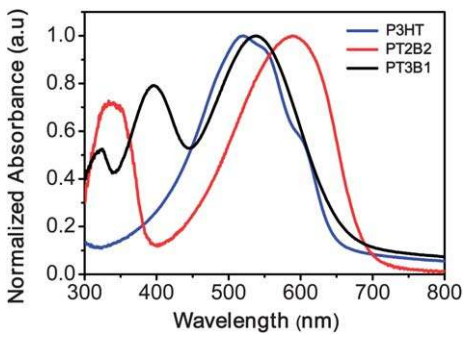

Fig. 2 Normalized UV-vis spectrum of **P3HT**, **PT3B1** and **PT2B2** thin film layer deposited on glass from chloroform solution.

2.3 Electrochemical properties

The electrochemical properties of the thiophene–benzothiadiazole based copolymers were examined by cyclic voltammetry (CV). Using this technique the energy levels of the copolymer such as HOMO and LUMO can be determined. These energy levels are crucial for the selection of appropriate acceptor materials in OPV blends. CV measurements were carried out in a 0.1 M tetrabutylammonium tetrafluoroborate (Bu_4NBF_4) solution in acetonitrile at room temperature using a scan rate of 50 mV s^{-1} under nitrogen. A Pt electrode coated with the polymer film by drop casting was used as working electrode and the Ag/AgCl electrode was used as reference electrode. The HOMO and LUMO levels of the copolymer were calculated from the oxidation and reduction onset potential relative to ferrocene as an internal standard, by treating the ionisation potential as −4.8 eV for the ferrocene/ferrocenium (Fe/Fe^+) redox system. The onset potentials were determined from the intersection of two tangents drawn as the rising current and baseline charging current of the CV traces. The electrochemical data for the two copolymers are shown in Fig. 3 and summarized in Table 2. Both copolymers exhibited a predominant oxidation peak (anodic peak) due to the electron donating oligothiophene units and a slight reduction peak related with the electron withdrawing benzothiadiazole moiety. The oxidation onsets for **PT3B1** and **PT2B2** copolymers were observed at 1.08 V and 1.28 V relative to ferrocene, respectively. Using these values, HOMO energy levels (E_{HOMO}) for **PT3B1** and **PT2B2** copolymers were calculated as 5.20 eV and 5.40 eV, respectively. LUMO values for **PT3B1** and **PT2B2** were 3.24 eV and 3.60 eV,

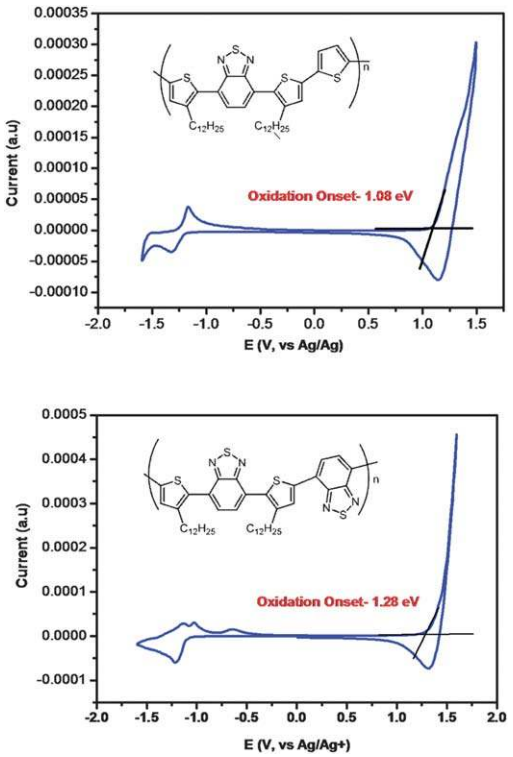

Fig. 3 Cyclic voltammograms showing the first scan of cathodic and anodic cycles of **PT3B1** and **PT2B2** spin coated polymers on working electrode at a scan rate 50 mV s^{-1} in acetonitrile. The electrolyte was 0.1 M $TBAPF_6$.

calculated from the difference between optical band gap and HOMO values. The polymer **PT2B2** shows a lower lying HOMO level than **PT3B1**, this is due to shifting of the LUMO further away from vacuum caused by the stabilization effect due to the two electron-withdrawing benzothiadiazole moieties in the polymer backbone.[19] Due to the higher number of thiophenes in **PT3B1** (increased donor nature), the HOMO level is higher than **PT2B2**. As expected, **PT2B2** shows a lower LUMO level than **PT3B1** which can be correlated to the higher content of benzothiadiazole units.[19] These studies confirm that the composition of donor and acceptor moieties in the polymeric backbone can alter the energy levels. An energy level diagram of the OPV device structure using these new donor polymers (**PT3B1** and **PT2B2**) and the PCBM acceptor is shown in Fig. 4 with references to the vacuum level.

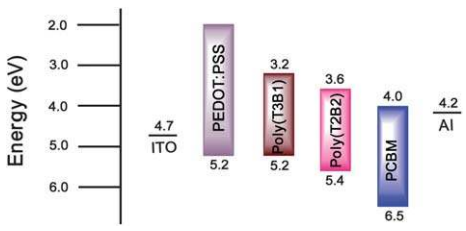

Fig. 4 Energy level diagram of OPV device structure using new donor polymers (**PT3B1** and **PT2B2**) and PCBM acceptor references to the vacuum level.

2.4 Organic field-effect transistors (OFETs)

Polymer OFETs were fabricated using bottom gate top contact device geometry with 40–50 nm solution processed thin films of **PT3B1** and **PT2B2** channel semiconductors. Out of the two polymers, only **PT3B1** exhibited p-channel OFET behaviour whereas polymer **PT2B2** did not show any channel conductance. In our earlier study for small molecule donor–acceptor systems, we also did not observe OFET performance for the **T2B2** small molecule whereas for **T3B1** we observed a mobility of 2.0×10^{-2} cm^2 V^{-1} s^{-1}.[14b] One of the possibilities for no charge accumulation of **PT2B2** thin film in OFET devices could be related with the structural disorder at the semiconductor/dielectric interface leading to charge trapping. The output and transfer characteristics of OFETs using **PT3B1** channel semiconductor are shown in Fig. 5. The devices exhibit p-channel performance with the mobility, calculated from the saturation regime, of 6.1×10^{-4} cm^2 V^{-1} s^{-1} and threshold voltage of −15.5 Volts. The OFET devices fabricated on OTS treated Si/SiO_2 substrates have shown more than one order of magnitude higher hole mobility as compared to the transistors fabricated on bare Si/SiO_2 substrates ($\mu_h = 3.0 \times 10^{-5}$ cm^2 V^{-1} s^{-1}). Higher hole mobility exhibited in OFET devices fabricated on OTS treated substrates can be attributed to better packing of **PT3B1** polymer thin films on SAM treated substrates.[20] This mobility values are within the range of previously reported thiophene–benzothiadiazole based copolymers.[21]

2.5 Organic photovoltaic (OPV) devices

Organic photovoltaic devices were made utilizing either **PT3B1** or **PT2B2** as the donor material, paired with [70]PCBM as the acceptor (note, devices utilizing [60]PCBM instead showed a much reduced short circuit current, suggesting significant photocurrent can be attributed to absorption by [70]PCBM and subsequent hole transfer to the polymer). The donor–acceptor ratio and thickness were varied for the optimization of devices in an attempt to maximum device performance. Devices made with a 1 : 4 ratio demonstrated better performance than devices with 1 : 1 or 1 : 2 ratios, for both donor polymers. An active layer thickness around 60 nm proved optimal and the highest achieved power conversion efficiencies were 2.54% and 1.06% for **PT3B1** and **PT2B2**-based devices, respectively. Current density–voltage curves for 1 : 4 ratio devices of varied thickness, under

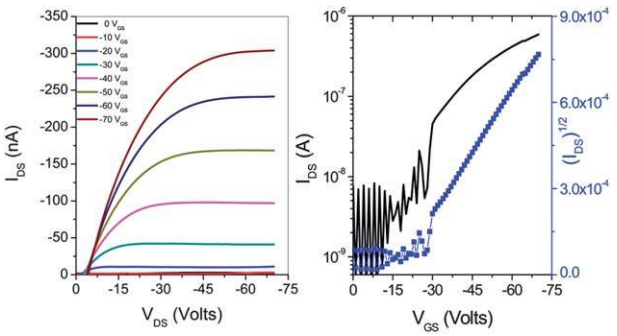

Fig. 5 (a) Output (VGS = 0 V to −70 V) and (b) transfer (VDS = −70 V) characteristics of OTFTs with **PT3B1** thin films.

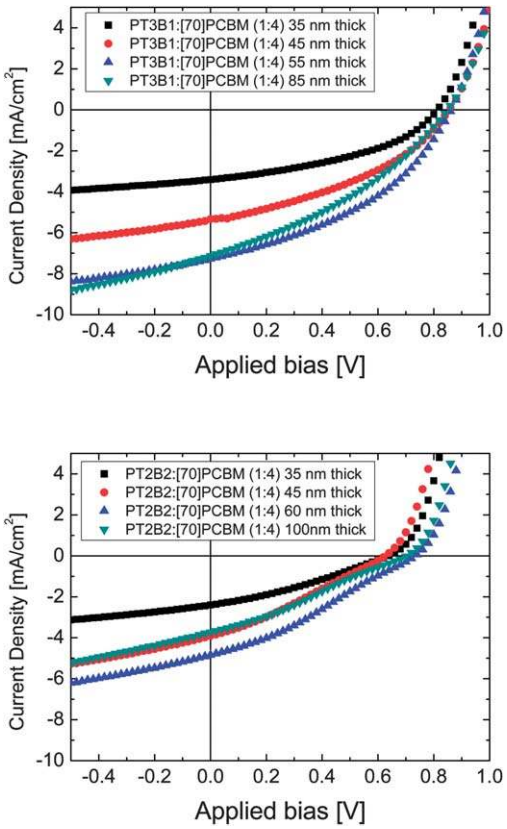

Fig. 6 Current density–voltage curves for various thicknesses of **PT3B1** and **PT2B2** devices, as blended with [70]PCBM in a 1 : 4 ratio.

illumination, are shown in Fig. 6, and solar cell characteristics are summarized in Table 3.

Devices employing **PT3B1** showed significantly higher J_{sc} values than devices with **PT2B2**. The lower lying LUMO level of **PT2B2** suggests that exciton dissociation by the fullerene may not be as efficient as in the **PT3B1** case, yielding less photocurrent. The V_{oc} of organic photovoltaic devices is often correlated with the difference between the donor HOMO level and the acceptor LUMO level from which holes and electrons, respectively, are extracted. Despite the lower lying HOMO level of **PT2B2**, devices incorporating this polymer displayed a lower V_{oc} than devices using **PT3B1**. Recombination of charge carriers is known to adversely affect the V_{oc}, and the very low fill factor for **PT2B2** devices may also be indicative of significant recombination. Although slightly higher, close to 40%, the fill factor for **PT3B1** devices suggests that charge transport of electrons and holes may not be balanced for OPV devices employing either of these donor polymers.

PT2B2-based devices show a pronounced kink in the *J–V* curve, as can be seen for all thicknesses of 1 : 4 blend ratio devices in Fig. 6. Although not shown, it should be noted that this kink was evident at 1 : 1 and 1 : 2 blend ratios, as well. A kink in the *J–V* curve has been observed in a range of solar cell systems,[22–24] including CIGS, DSSC, and a number of organic photovoltaics, and with a variety of characteristics and shapes. It is commonly and generally attributed to an interfacial effect and/or poor or unbalanced charge carrier collection. It is interesting to note that the kink displayed here is predominantly a 4th quadrant characteristic; detailed evaluation of this kink is beyond the scope of this paper and will be discussed elsewhere.

A strong dependence of performance on active layer thickness is clearly evident from examination of the cells' J_{sc} values. It is of interest to look at the IPCE spectra with thickness for these devices in Fig. 7. A clear change in shape occurs over a fairly small change in thickness, as revealed by **PT3B1** : [70]PCBM (1 : 4) devices of 45, 55, and 85 nm. A similar trend with thickness is observed for **PT2B2** devices. The significant amount of overlap between the absorption spectra of the donor polymers and [70]PCBM makes it difficult to unequivocally attribute changes to primarily the donor or acceptor. Qualitatively, the thinnest devices have a more pronounced blue response, while thicker devices show a more significant red response. Optical absorption measurements revealed spectra that closely resembled that of the fullerene, which might be expected given the 1 : 4 ratio in composition. Optical interference effects have been known to influence device performance, but it would seem unlikely that such relatively small changes in thickness could result in these significant changes over such a broad spectral range. Morphological effects, changes in donor–acceptor segregation and intermixing, may be playing an important role in determining the IPCE spectra. Likewise, possible differences in blend morphology, between **PT3B1** devices and **PT2B2** devices, make it difficult to ascertain the extent of the role of the varied energy levels on device performance.

Table 3 Summary of photovoltaic device performance

Donor	Acceptor	Ratio	Thickness/nm	J_{sc}/mA cm^{-2}	V_{oc}/V	FF (%)	PCE (%)
PT2B2	[70]PCBM	1 : 4	30	2.4	0.64	31	0.48
PT2B2	[70]PCBM	1 : 4	40	3.9	0.63	28	0.7
PT2B2	[70]PCBM	*1 : 4*	*60*	*4.8*	*0.73*	*30*	*1.06*
PT2B2	[70]PCBM	1 : 4	100	3.7	0.70	28	0.73
PT2B2	[70]PCBM	1 : 1	60	1.7	0.73	21	0.26
PT2B2	[70]PCBM	1 : 2	65	3.9	0.74	25	0.73
PT2B2	[60]PCBM	1 : 4	60	0.93	0.71	27	0.18
PT3B1	[70]PCBM	1 : 4	35	3.4	0.81	42	1.15
PT3B1	[70]PCBM	1 : 4	45	5.33	0.85	39	1.79
PT3B1	[70]PCBM	*1 : 4*	*55*	*7.27*	*0.86*	*41*	*2.54*
PT3B1	[70]PCBM	1 : 4	85	7.13	0.85	35	2.12
PT3B1	[70]PCBM	1 : 1	60	1.5	0.88	24	0.32
PT3B1	[70]PCBM	1 : 2	60	5.6	0.93	33	1.7
PT3B1	[60]PCBM	1 : 4	60	3.3	0.78	34	0.88

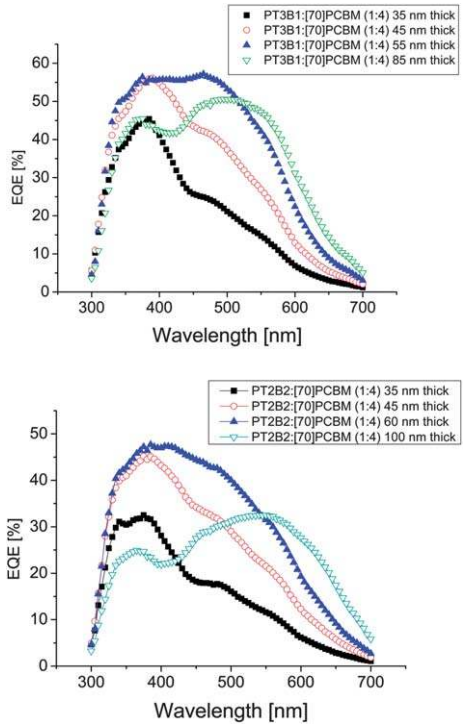

Fig. 7 IPCE spectra of **PT3B1** and **PT2B2** devices, as blended with [70] PCBM in a 1 : 4 ratio.

3. Conclusion

Novel push–pull thiophene–benzothiadiazole–thiophene (D–A–D) based low band gap organic semiconducting copolymers have been designed, synthesized and characterized. The effect of a donating or accepting moiety adjacent to the thiophene–benzothiadiazole–thiophene (D–A–D) segment on optical properties, energy levels, and performances in OFET and OPV devices has been investigated. Solution processed thin film photovoltaic devices utilizing the corresponding donor polymers with a PCBM acceptor exhibited promising performance. A highest power conversion efficiency of 2.54% has been achieved for devices using **PT3B1** donor polymer with [70]PCBM as the acceptor. These findings suggest that the careful design of D–A–D blocks in the polymer backbone can alter the photophysical properties.

4. Experimental

General

All the chemicals were purchased from Strem, Acros and Sigma-Aldrich and used without further purification. All reactions were carried out using Schlenk techniques in an argon or nitrogen atmosphere with anhydrous solvents.

Characterization

^{1}H and ^{13}C NMR data were performed on a Bruker DPX 400 MHz spectrometer with chemical shifts referenced to residual $CHCl_3$ and H_2O in $CDCl_3$. Matrix assisted laser desorption/ionization time-of-flight (MALDI-TOF) mass spectra were obtained on a Bruker Autoflex TOF/TOF instrument using dithranol as a matrix. GPC analysis against PS standards was performed in THF on a Waters high pressure GPC assembly with separation model 2690 and Evaporative Light Scattering (ELS 2420) detector. The pore sizes of 3 Phenogel columns in use are 10^6, 10^4, and 500 Å. The flow rate of THF is 1 mL min^{-1} and column oven temperature is 40 °C. A typical concentration 1.5 mg weight of polymer dissolved in 1 mL of THF was used for running GPC samples. UV-Vis spectra were recorded on a Shimadzu model 2501-PC. Photoluminescence (PL) spectra were measured on a Perkin-Elmer (LS50B) spectrofluorimeter. Cyclic voltammetry experiments were performed using an Autolab potentiostat (model PGSTAT30) by Echochimie. All CV measurements were recorded in solid state with 0.1 M tetrabutylammonium hexafluorophosphate as the supporting electrolyte (scan rate of 50 mV s^{-1}). The experiments were performed at room temperature with a conventional three-electrode configuration consisting of a platinum disc working electrode, a gold counter electrode, and an Ag/AgCl reference electrode. Differential scanning calorimetry (DSC) was carried out under nitrogen on a TA Instrument DSC Q100 (scanning rate of 10 °C min^{-1}). Thermal gravimetric analysis (TGA) was carried out using a TA Instrument TGA Q500 (heating rate of 10 °C min^{-1}).

Synthesis of 2-bromo-3-dodecylthiophene (2). To a solution of 3-dodecylthiophene (5.00 g, 19.8 mmol) in the mixture of $CHCl_3$ (20 mL) and CH_3COOH (20 mL) *N*-bromosuccinamide (NBS) (3.52 g 19.8 mmol) was added portion wise over a period of 1 h. The reaction mixture was stirred overnight at room temperature. After completion of the reaction it was then poured into water and extracted with chloroform. The combined organic phase was washed with chloroform, brine solution and dried over magnesium sulfate. After filtration, the chloroform was removed on a rotavap and the crude product was purified by column chromatography using hexane as the solvent (6.00 g, 93%).

^{1}H NMR (400 MHz, $CDCl_3$, ppm): δ = 0.88 (t, 3H, CH_3, J = 6.7 Hz), 1.29 (m, 18H, 9CH_2), 1.62 (q, 2H, CH_2, J = 7.2 Hz, J= 7.2 Hz), 2.55 (t, 2H, CH_2, J = 7.5 Hz), 6.77 (d, 2H, Th, J = 5.8 Hz), 7.18 (d, 2H, Th, J = 5.8 Hz).

Synthesis of 2-tributylstannyl-3-dodecylthiophene (3). Magnesium turnings (0.400 g 16.6 mmol) in anhydrous THF (15.0 mL) were heated to mild reflux until totally disappearing. This solution was added drop wise to the solution of 2-bromo-3-dodecylthiophene (5.0 g, 15 mmol) in 15 mL of THF. The reaction mixture was refluxed for 2 h before being transferred to a solution of tributyltin chloride (4.50 mL, 16.02 mmol) in 25 mL of anhydrous THF at −78 °C. The mixture was allowed to warm to room temperature and stirred overnight before pouring into water. The aqueous layer was extracted with hexanes, and the combined organic phase was washed with brine and dried over $MgSO_4$. The crude compound was used as such for the next step (5.00 g, 61%).

^{1}H NMR (400 MHz, $CDCl_3$): δ = 0.89–1.60 (m, 50H, 4CH_3, 19CH_2), 2.63 (t, 2H, CH_2, J = 7.8 Hz), 7.11 (d, 1H, Th, J = 4.8 Hz), 7.54 (d, 2H, Th, J = 4.8 Hz).

Synthesis of 4,7-bis(3-dodecylthiophene-2-yl)benzo[*c*][1,2,5]-thiadiazole (5). 2-(Trimethylstannyl)-3-dodecylthiophene (4.50 g,

10. 60 mmol) and 4,7-dibromobenzothiadiazole (1.06 g, 3.62 mmol) were dissolved in dry DMF (50 mL). Then Pd $(PPh_3)_4$ (0.125 g, 3 mol%) was added to the above reaction mixture under argon and heated to reflux at 110 °C for 48 hours. The mixture was allowed to cool to room temperature and poured into water. The aqueous layer was extracted with dichloromethane, and the combined organic phase was washed with brine and dried over $MgSO_4$. The crude product was purified by column chromatography using hexane : DCM as eluent (1.5 g, 65%).

^{1}H NMR (400 MHz, $CDCl_3$): δ = 0.88 (t, 3H, CH_3, J = 6.8 Hz), 1.23 (m, 18H, CH_2), 1.63 (q, 2H, CH_2, J = 7.8 Hz, J = 7.4 Hz), 2.67 (t, 2H, CH_2, J = 7.5 Hz), 7.11(d, 2H, Th, J = 5.4 Hz), 7.45 (d, 2H, Th, J = 5.3 Hz), 7.63(s, 1H, btz).

MALDI-TOF-MS (dithranol) m/z: 635.68 (M^+); calcd for $C_{38}H_{56}N_2S_3$ = 636.36.

Synthesis of 4,7-bis(5-bromo-3-dodecylthiophen-2-yl)benzo[*c*]-[1,2,5]thiadiazole (6). 4,7-Bis(3-dodecylthiophene-2-yl)benzo[*c*][1,2,5]thiadiazole (1.27 g 2.00 mmol) was dissolved in 25 mL dimethylformamide (DMF) under argon in the absence of light. *N*-Bromosuccinamide (NBS) (0.90 g 5.040 mmol) was dissolved in another 25 mL dimethylformamide (DMF) and added drop wise through a dropping funnel to the above reaction mixture. The resulting reaction mixture was stirred overnight at room temperature. The reaction was worked up by pouring the reaction mixture into water and extracting the aqueous layer with dichloromethane, and the combined organic phase was washed with brine and dried over $MgSO_4$. The crude compound was purified by column chromatography using hexane : DCM as eluent (1.0 g, 62%).

^{1}H NMR (400 MHz, $CDCl_3$): δ = 0.89 (t, 3H, CH_3, J = 6.7 Hz), 1.23 (m, 18H, CH_2), 1.61 (q, 2H, CH_2, J = 6.8 Hz, J = 8.3 Hz), 2.64 (t, 2H, CH_2, J = 7.5 Hz), 7.06 (s, 1H, Th), 7.60 (s, 1H, btz). ^{13}C NMR (100 MHz, $CDCl_3$, ppm): δ = 154.33, 142.89, 134.00, 132.380, 130.05, 127.09, 113.54, 32.27, 30.85, 29.97, 29.81, 29.69, 23.02, 14.42.

MALDI-TOF-MS (dithranol) m/z: 793.59(M + 1); calcd for $C_{38}H_{54}Br_2N_2S_3$ = 792.18. Anal. Calcd for $C_{38}H_{54}Br_2N_2S_3$: C, 57.42; H, 6.85; N, 3.52; S, 12.10%. Found: C, 57.38; H, 6.79; N, 3.46; S, 12.25%.

Synthesis of 2,5-bis(trimethylstannyl)thiophene (7). A hexane solution of butyllithium (1.6 M, 30 mmol, 19 mL) was added to a THF (50 mL) solution of thiophene (1.26 g, 15 mmol) at −78 °C. Upon formation of white precipitate, the mixture was warmed to rt and stirred for 1 h followed by addition of trimethyltin chloride. The clear solution was heated to gentle reflux for 1 h, and it turned cloudy. The reaction mixture was poured into water. The organic layer was separated and dried over $MgSO_4$. After removal of the solvent by evaporation, the residue was recrystallized 3 times from isopropanol to obtain the title compound (3.9 g, 60%).

^{1}H NMR (400 MHz, $CDCl_3$): δ = 0.37 (s, 18H), 7.38 (s, 2H). ^{13}C NMR (100 MHz, $CDCl_3$, ppm): δ = −7.86, 136.21, 144.42.

MALDI-TOF-MS (dithranol) m/z: = 408, 410, 412 (M^+, three most intense peaks of the isotope pattern); calcd for $C_{10}H_{20}SSn_2$ = 411.93. Anal. Calcd for $C_{10}H_{20}SSn_2$: C, 29.31; H, 4.92; S, 7.83%. Found: C, 29.25; H, 4.98; S, 7.75%.

Synthesis of 4,7-bis(4,4,5,5-tetramethyl-1,3,2-dioxaborolan-2-yl)benzo[*c*][1,2,5]thiadiazole (8). 4,7-Dibromo-2,1,3-benzothiadiazole (**5**) (4.0 g, 13.6 mmol), bis(pinacolato)diboron (8.0 g, 31.2 mmol), $PdCl_2$(dppf) (2.0 g, 2.4 mmol), and KOAc (8.0 g, 80 mmol) were kept under vacuum for 10 min and then degassed before 1,4-dioxane (50 mL) was added under argon. The reaction mixture was stirred at 80 °C overnight and quenched by adding water. The resulting mixture was extracted with ethyl acetate (100 mL). The combined organic layers were washed with brine, dried over Na_2SO_4, and filtered. After removing the solvent, a dark red solid was obtained, which was purified by silica gel chromatography by using 3% ethyl acetate in hexane as eluent to give the title compound as a pink solid (2.4 g, 46%).

^{1}H NMR (400 MHz, $CDCl_3$): δ = 8.12 (s, 2H), 1.43 (s, 24H). ^{13}C NMR (100 MHz, $CDCl_3$, ppm): δ = 157.55, 138.11, 84.91, 25.3.

MALDI-TOF-MS (dithranol) m/z: = 388.0; calcd for $C_{18}H_{26}B_2N_2O_4S$ = 388.18. Anal. Calcd for $C_{18}H_{26}Br_2N_2O_4S$: C, 55.71; H, 6.75; N, 7.22; S, 8.26%. Found: C, 55.65; H, 6.82; N, 7.16; S, 8.15%.

Synthesis of poly[4,7-bis(3-dodecylthiophene-2-yl) benzothiadiazole-*co*-thiophene] (PT3B1). To a 50 mL Schlenk flask, 4,7-bis (5-bromo-3-dodecylthiophen-2-yl)benzo[*c*][1,2,5]thiadiazole **6** (0.400 g, 0.50 mmol) and 2,5-bis(trimethylstannyl)thiophene (0.207 g, 0.50 mmol), tris(dibenzylideneacetone)dipalladium(0) (9.14 mg, 0.001mmol), tri(*o*-tolyl)phosphine (12.16 mg, 0.04 mmol), and anhydrous chlorobenzene (20 mL) were charged. The solution was purged with argon for 30 min, and then the reaction mixture was stirred at 80 °C for 2 d. On the third day, 0.5 mL of bromobenzene was added to the reaction mixture to react with the unreacted trimethylstannyl end groups. The mixture was further stirred at 80 °C for 6 h before cooling down to room temperature, and poured into 200 mL of stirring methanol. The solid was filtered off, washed with methanol, and dried. The solid was further purified by Soxhlet extraction using acetone, methanol and hexane, respectively, and then finally dissolved with chloroform. A dark red, shiny, metallic solid was obtained after removing the solvent and precipitating in methanol (0.365 g, 97%). M_w/M_n (GPC) = 56 180/31,170. UV-vis: 384 and 500 nm (in chloroform); 395 and 539 nm (thin film).

^{1}H NMR (400 MHz, $CDCl_3$, δ): 0.88 (m, 3H, CH_3), 1.26 (m, 18H), 1.70 (m, 2H), 2.72 (m, 2H), 7.10–7.30 (br, 2H), 7.71 (s, 1H).

Synthesis of poly[4,7-bis(3-dodecylthiophene-2-yl) benzothiadiazole-*co*-benzothiadiazole] (PT2B2). To a Schlenk flask, 4,7-bis (5-bromo-3-dodecylthiophen-2-yl)benzo[*c*][1,2,5]thiadiazole **6** (0.300 g, 0.37 mmol) and 4,7-bis(4,4,5,5-tetramethyl-1,3,2-dioxabrolan-2-yl)benzothiadiazole (0.150 g, 0.37 mmol), 2 M aqueous K_2CO_3 solution (5 mL) and 2 drops of Aliquat 336 were dissolved in toluene (10 mL). The solution was purged with argon for 30 min, and then tetrakis(triphenylphosphine)palladium (13 mg, 0.011 mmol) was added. The reaction was stirred at 80 °C for 3 d. Then a toluene solution of phenyl boronic acid was added and the mixture was stirred for additional 4 h, followed by addition of a few drops of bromobenzene and stirred overnight. The resulting mixture was poured into a mixture of methanol and water and stirred overnight. The dark precipitate was re-dissolved in chloroform and added drop wise to methanol (250 mL).

The resulting solid was filtered off and subjected to Soxhlet extraction for 2 d in methanol, acetone, and hexane for the removal of oligomers and catalytic impurities. The remaining polymer was extracted with chloroform and precipitated again from methanol, filtered, washed with methanol, and dried under vacuum at room temperature (0.300 g, 69% yield). M_w/M_n (GPC) = 8490/11 560. UV-vis: 320, 521 nm (in chloroform); 338, 589 nm (thin film).

^{1}H NMR (400 MHz, $CDCl_3$, δ): 0.87 (m, 3H, CH_3), 1.20–1.35 (m, 18H), 1.78 (m, 2H), 2.84 (m, 2H), 7.80 (s, 1H), 7.93 (s, 1H), 8.20 (s, 1H).

OFET fabrication and characterization. Top contact/bottom gate OTFT devices were fabricated using p^+-Si/SiO_2 substrates where p^+-Si and SiO_2 work as gate electrode and gate dielectric, respectively. Substrates were subjected to cleaning using ultrasonication in acetone, methanol and de-ionized water. The cleaned substrates were dried under a nitrogen flow and heated at 100 °C for 5 min. The substrates were then treated in UV-ozone for 20 min. Then, the substrate was kept in a desiccator with a few drops of octyltrichlorosilane (OTS). The desiccator was evacuated for 3 min and placed in an oven at 110 °C for 3 h. The substrate was removed from the desiccator, thoroughly rinsed with isopropanol, and dried under a nitrogen flow. **PT3B1** thin film was spin cast using 8 mg mL^{-1} solution in chloroform on the OTS treated Si/SiO_2 substrate. Subsequently, on top of the polymer active layer, a roughly 100 nm thick gold (Au) thin film was deposited for source (*S*) and drain (*D*) electrodes through a shadow mask. For a typical OTFT device reported here, the source–drain channel length (*L*) and channel width (W) were 100 μm and 3 mm, respectively. The device characteristics of the OFETs were measured at room temperature under nitrogen with a Keithley 2400 source meter. The field effect mobility (μ) was calculated from the saturation regime of transfer characteristics.

OPV fabrication and its characterization. For solar cell device fabrication, patterned indium tin oxide (ITO)-coated glass substrates were purchased from Kintec. The glass/ITO substrates were cleaned by ultrasonication in subsequent baths of detergent (15 min), de-ionized water (15 min), acetone (15 min), methanol (15 min) and isopropanol (15 min). The substrates were then dried at 80 °C for several hours in an oven to remove residual solvents. The substrates were the subjected to oxygen plasma cleaning for 10 minutes prior to the spin coating of a 40 nm thick PEDOT:PSS hole transporting layer (Clevios P VP AI 4083). The active layer of **PT3B1** : [70]PCBM or **PT2B2** : [70]PCBM in varied ratios and concentrations was spin coated to obtain a range of thicknesses. An aluminium cathode was deposited by thermal evaporation through a shadow mask under a pressure of roughly 10^{-5} mbar to complete the devices, having device square area of 9 mm^2. The IPCE (Incident Photon-to-current Conversion Efficiency) was measured with a testing system consisting of an Oriel 300 W Xe lamp in combination with a monochromator (Oriel Cornerstone 130), and lock-in amplifier (Stanford Research Systems, SRS 810); the incident light intensity was determined by a calibrated Si photodiode. The current–voltage characteristics were measured using a source meter (Keithley 2400), while irradiance was provided by a solar simulator (Steuernagel, Germany model 535). The simulator lamp intensity was set using a reference cell (Hamamatsu S1787-04) and the calculated spectral mismatch factor.

Acknowledgements

The authors acknowledge the Visiting Investigatorship Programme (VIP) of the Agency for Science, Technology and Research (A*STAR), Republic of Singapore, for financial support. We are also thankful to Chua Pei Lin and Pang Lusha from Republic Polytechnic, Singapore, for scaling up starting precursors during their attachment program with IMRE.

References

1 (*a*) Y. Shirota and H. Kageyama, *Chem. Rev.*, 2007, **107**, 953; (*b*) H. Klauk, *Organic Electronics: Materials Manufacturing and Applications*, Wiley, Weinheim, 2006; (*c*) K. Müllen and G. Wegner, *Electronic Materials: The Material Approach*, Wiley-VCH, Weinheim, 1998.

2 (*a*) J. Kido and Y. Okamoto, *Chem. Rev.*, 2002, **102**, 2357; (*b*) A. C. Grimsdale, K. L. Chan, R. E. Martin, P. G. Jokisz and A. B. Holmes, *Chem. Rev.*, 2009, **109**, 897.

3 (*a*) A. Facchetti, *Mater. Today*, 2007, **10**, 28; (*b*) B. S. Ong, Y. Wu, Y. Li, P. Liu and H. Pan, *Chem.–Eur. J.*, 2008, **14**, 4766; (*c*) S. Allard, M. Forster, B. Souharce, H. Thiem and U. Scherf, *Angew. Chem., Int. Ed.*, 2008, **47**, 2.

4 (*a*) *Organic Photovoltaics*, ed. C. Brabec, V. Dyakonov and U. Scherf, Wiley-VCH, Weinheim, Germany, 2008; (*b*) A. R. Murphy and J. M. J. Fréchet, *Chem. Rev.*, 2007, **107**, 1066.

5 (*a*) J. Roncali, *Chem. Rev.*, 1997, **97**, 173; (*b*) B. Tieke, A. R. Rabindranath, K. Zhang and Y. Zhu, *Beilstein J. Org. Chem.*, 2010, **6**, 830; (*c*) Y. J. He and Y. F. Li, *Progr. Chem.*, 2009, **21**, 2303; (*d*) W. Z. Cai, X. Gong and Y. Cao, *Sol. Energy Mater. Sol. Cells*, 2010, **94**, 114.

6 (*a*) J. Chen and Y. Cao, *Acc. Chem. Res.*, 2009, **42**, 1709; (*b*) T. Yamamoto, *Macromol. Rapid Commun.*, 2002, **23**, 583; (*c*) J. Roncali, *Chem. Rev.*, 1992, **92**, 711.

7 (*a*) P. Sonar, S. P. Singh, Y. Li, M. S. Soh and A. Dodabalapur, *Adv. Mater.*, 2010, **22**, 5409; (*b*) L. Bürgi, M. Turbiez, R. Pfeiffer, F. Bienewald, H.-J. Kirner and C. Winnewisser, *Adv. Mater.*, 2008, **20**, 2217; (*c*) J. C. Bijleveld, A. P. Zoombelt, S. G. J. Mathijssen, M. M. Wienk, M. Turbiez, D. M. de Leeuw and R. A. J. Janssen, *J. Am. Chem. Soc.*, 2009, **131**, 16616; (*d*) J. C. Bijleveld, V. S. Gevaerts, D. D. Nuzzo, M. Turbiez, S. G. J. Mathijssen, D. M. de Leeuw, M. M. Wienk and R. A. J. Janssen, *Adv. Mater.*, 2010, **22**, 242; (*e*) M. M. Wienk, M. Turbiez, J. Gilot and R. A. J. Janssen, *Adv. Mater.*, 2008, **20**, 2556; (*f*) T. L. Nelson, T. M. Young, J. Liu, S. P. Mishra, J. A. Belot, C. L. Balliet, A. E. Javier, T. Kowalewski and R. D. McCullough, *Adv. Mater.*, 2010, **22**, 4617.

8 (*a*) M. Jayakannan, P. A. Van Hal and R. A. J. Janssen, *J. Polym. Sci., Part A: Polym. Chem.*, 2001, **40**, 251; (*b*) E. Wang, L. Wang, L. Lan, C. Luo, W. Zhuang, J. Peng and Y. Cao, *Appl. Phys. Lett.*, 2008, **92**, 033307; (*c*) P.-L. T. Boudreault, A. Michaud and M. Leclerc, *Macromol. Rapid Commun.*, 2007, **28**, 2176.

9 (*a*) A. J. Moulé, A. Tsami, T. W. Bünnagel, M. Forster, N. M. Kronenberg, M. Scharber, M. Koppe, M. Morana, C. J. Brabec, K. Meerholz and U. Scherf, *Chem. Mater.*, 2008, **20**, 4045; (*b*) N. Blouin, A. Michaud and M. Leclerc, *Adv. Mater.*, 2007, **19**, 2295; (*c*) N. Blouin, A. Michaud, D. Gendron, S. Wakim, E. Blair, R. Neagu-Plesu, M. Belletête, G. Durocher, Y. Tao and M. Leclerc, *J. Am. Chem. Soc.*, 2008, **130**, 732.

10 (*a*) L. H. Slooff, S. C. Veenstra, J. M. Kroon, D. J. D. Moet, J. Sweelssen and M. M. Koetse, *Appl. Phys. Lett.*, 2007, **90**, 143506; (*b*) D. Veldman, Ö. Pek, S. C. J. Meskers, J. Sweelssen, M. M. Koetse, S. C. Veenstra, J. M. Kroon, S. S. van Bavel, J. Loos and R. A. J. Janssen, *J. Am. Chem. Soc.*, 2008, **130**, 7721; (*c*) M. Svensson, F. Zhang, S. C. Veenstra, W. J. H. Verhees, J. C. Hummelen, J. M. Kroon, O. Inganas and M. R. Andersson, *Adv. Mater.*, 2003, **15**, 988; (*d*) O. Inganäs, M. Svensson, F. Zhang, A. Gadisa, N. K. Persson, X. Wang and M. R. Andersson, *Appl. Phys. A: Solids Surf.*, 2004, **79**, 31.

11 (*a*) Q. Zheng, B. Jun, J. Sun and H. E. Katz, *J. Am. Chem. Soc.*, 2010, **132**, 5394; (*b*) L. Biniek, C. L. Chochos, N. Leclère, G. Hadziionnou, J. K. Kallitsis, R. Bechara, P. Lèvêque and T. Heiser, *J. Mat. Chem.*, 2009, **19**, 4946; (*c*) L. Biniek, C. L. Chochos, G. Hadziioannou, N. Leclerc, P. Lèvêque and T. Heiser, *Macromol. Rapid Commun.*, 2010, **31**, 651.

12 (*a*) E. Bundgaard and F. C. Krebs, *Macromolecules*, 2006, **39**, 2823; (*b*) E. Bundgaard and F. C. Krebs, *Sol. Energy Mater. Sol. Cells*, 2007, **11**, 954; (*c*) E. Bundgaard and F. C. Krebs, *Sol. Energy Mater. Sol. Cells*, 2007, **91**, 1019; (*d*) J. E. Carlè, J. W. Andreasen, M. Jorgensen and F. C. Krebs, *Sol. Energy Mater. Sol. Cells*, 2010, **94**, 774.

13 (*a*) Y. Yamashita, *Chem. Lett.*, 2009, **38**, 870; (*b*) K. Imaeda, Y. Yamashita, Y. Li, T. Mori, H. Inokuchi and M. Sano, *J. Mater. Chem.*, 1992, **2**, 115; (*c*) P. Gao, PhD dissertation, University of Mainz, Germany, 2010; (*d*) G. J. McEntee, F. Vilela, P. J. Skabara, T. D. Anthopoulos, J. G. Labram, S. Tierney, R. W. Harrington and W. Clegg, *J. Mater. Chem.*, 2011, **21**, 2091; (*e*) H. Pang, P. J. Skabara, D. J. Crouch, W. Duffy, M. Henney, I. McCulloch, S. J. Coles, P. N. Horton and M. B. Hursthouse, *Macromolecules*, 2007, **40**, 6585; (*f*) H. Pang, F. Viela, P. J. Skabara, J. J. W. McDouall, D. J. Crouch, T. D. Anthopoulos, D. D. C. Bradley, D. M. de Leeuw, P. N. Horton and M. B. Hursthouse, *Adv. Mater.*, 2007, **19**, 4438; (*g*) T. Yasuda, T. Imase, S. Sasaki and T. Yamamoto, *Macromolecules*, 2005, **38**, 1500.

14 (*a*) P. Sonar, S. P. Singh, S. Sudhakar, A. Dodabalapur and A. Sellinger, *Chem. Mater.*, 2008, **9**, 3184; (*b*) P. Sonar, S. P. Singh, P. Leclère, M. Surin, R. Lazzaroni, T. T. Lin, A. Dodabalapur and A. Sellinger, *J. Mat. Chem.*, 2009, **19**, 3228.

15 (*a*) *Printed Organic and Molecular Electronics*, ed. D. R. Gamota, P. Brazis, K. Kalyansundaram and J. Zhang, Kluwer Academic Publishers, 2004; (*b*) F. C. Krebs, *Sol. Energy Mater. Sol. Cells*, 2009, **93**, 394.

16 (*a*) Y. Wei, Y. Yang and J.-M. Yeh, *Chem. Mater.*, 1996, **8**, 2659; (*b*) M. Zhang, H. N. Tsao, W. Pisula, C. Yang, A. K. Mishra and K. Müllen, *J. Am. Chem. Soc.*, 2007, **129**, 3472.

17 (*a*) C. Shi, Y. Wu, W. Zeng, Y. Xie, K. Yang and Y. Cao, *Macromol. Chem. Phys.*, 2005, **206**, 1114; (*b*) M. Sendur, A. Balan, D. Baran, B. Karabay and L. Toppare, *Org. Electron.*, 2010, **11**, 1877.

18 (*a*) D. L. Pavia, G. M. Lampman and G. S. Kriz, *Introduction to Spectroscopy*, Saunders College Publishing, 2nd edn, 1996, ISBN: 0-03-058427-2; (*b*) M. F. Falzon, M. M. Wienk and R. A. J. Janssen, *J. Phys. Chem. C*, 2011, **115**, 3178; (*c*) H. Zhou, L. Yang, S. Stoneking and W. You, *ACS Appl. Mater. Interfaces*, 2010, **2**, 1377.

19 Two sp^2 hybridized nitrogen atoms in **PT2B2** polymer provide electron withdrawing effect and lead to a lowering of the LUMO energy level.

20 (*a*) F. F. Fan, J. Yang, L. Cai, D. W. Price, Jr, S. M. Dirk, D. V. Kosynkin, Y. Yao, A. M. Rawtlett, J. M. Tour and A. J. Bard, *J. Am. Chem. Soc.*, 2002, **124**, 5550; (*b*) I. Kymissis, C. D. Dimitrakopoulos and S. Purushothaman, *IEEE Trans. Electron Devices*, 2001, **48**, 1060; (*c*) A. Salleo, M. L. Chabinys, M. S. Yang and R. A. Street, *Appl. Phys. Lett.*, 2002, **81**, 4383.

21 W. Li, R. Qin, Y. Zhou, M. Andersson, F. Li, C. Zhang, B. Li, Z. Liu, Z. Bao and F. Zhang, *Polymer*, 2010, **51**, 3031.

22 (*a*) M. Glatthar, M. Riede, N. Keegan, K. Sylvester-Hvid, B. Zimmermann, M. Niggemann, A. Hinsch and A. Gombert, *Sol. Energy Mater. Sol. Cells*, 2007, **91**, 390; (*b*) J. F. Guillemoles, L. Kronik, D. Cahen, U. Rau, A. Jasenek and H. W. Schock, *J. Phys. Chem. B*, 2000, **104**, 4849; (*c*) D. Gupta, S. Mukopadhyay and K. S. Narayan, *Sol. Energy Mater. Sol. Cells*, 2010, **94**, 1309.

23 (*a*) J. M. Kroon, N. J. Bakker, H. J. P. Smit, P. Liska, K. R. Thampi, P. Wang, S. M. Zakeeruddin, M. Gratzel, A. Hinsch, S. Hore, U. Wurfel, R. Sastrawan, J. R. Durrant, E. Palomares, H. Petterson, T. Gruszecki, J. Walter, K. Skupien and G. E. Tulloch, *Prog. Photovoltaics*, 2007, **15**, 1; (*b*) A. Kumar, S. Sista and Y. Yang, *J. Appl. Phys.*, 2009, 105; (*c*) A. Wagenpfahl, D. Rauh, M. Binder, C. Deibel and V. Dyakonov, *Phys. Rev. B: Condens. Matter Mater. Phys.*, 2010, 82.

24 A. J. Moulé, J. B. Bonekamp and K. Meerholz, *J. Appl. Phys.*, 2006, **100**, 094503.